



Intel® Model: 18260NGW, FCC ID: PD918260NG

Intel® Model 18260NGW Embedded in Toshiba Model PT16B

RF Exposure Power Density and Evaluation Test Report

September 2016

Revision 1.1

Intel Confidential



Notice: This document contains information on products in the design phase of development. The information here is subject to change without notice. Do not finalize a design with this information.

INFORMATION IN THIS DOCUMENT IS PROVIDED IN CONNECTION WITH INTEL PRODUCTS. NO LICENSE, EXPRESS OR IMPLIED, BY ESTOPPEL OR OTHERWISE, TO ANY INTELLECTUAL PROPERTY RIGHTS IS GRANTED BY THIS DOCUMENT. EXCEPT AS PROVIDED IN INTEL'S TERMS AND CONDITIONS OF SALE FOR SUCH PRODUCTS, INTEL ASSUMES NO LIABILITY WHATSOEVER AND INTEL DISCLAIMS ANY EXPRESS OR IMPLIED WARRANTY, RELATING TO SALE AND/OR USE OF INTEL PRODUCTS INCLUDING LIABILITY OR WARRANTIES RELATING TO FITNESS FOR A PARTICULAR PURPOSE, MERCHANTABILITY, OR INFRINGEMENT OF ANY PATENT, COPYRIGHT OR OTHER INTELLECTUAL PROPERTY RIGHT.

A "Mission Critical Application" is any application in which failure of the Intel Product could result, directly or indirectly, in personal injury or death. SHOULD YOU PURCHASE OR USE INTEL'S PRODUCTS FOR ANY SUCH MISSION CRITICAL APPLICATION, YOU SHALL INDEMNIFY AND HOLD INTEL AND ITS SUBSIDIARIES, SUBCONTRACTORS AND AFFILIATES, AND THE DIRECTORS, OFFICERS, AND EMPLOYEES OF EACH, HARMLESS AGAINST ALL CLAIMS COSTS, DAMAGES, AND EXPENSES AND REASONABLE ATTORNEYS' FEES ARISING OUT OF, DIRECTLY OR INDIRECTLY, ANY CLAIM OF PRODUCT LIABILITY, PERSONAL INJURY, OR DEATH ARISING IN ANY WAY OUT OF SUCH MISSION CRITICAL APPLICATION, WHETHER OR NOT INTEL OR ITS SUBCONTRACTOR WAS NEGLIGENT IN THE DESIGN, MANUFACTURE, OR WARNING OF THE INTEL PRODUCT OR ANY OF ITS PARTS.

Intel may make changes to specifications and product descriptions at any time, without notice. Designers must not rely on the absence or characteristics of any features or instructions marked "reserved" or "undefined." Intel reserves these for future definition and shall have no responsibility whatsoever for conflicts or incompatibilities arising from future changes to them. The information here is subject to change without notice. Do not finalize a design with this information.

Intel software products are copyrighted by and shall remain the property of Intel Corporation. Use, duplication, or disclosure is subject to restrictions stated in Intel's Software License Agreement, or in the case of software delivered to the government, in accordance with the software license agreement as defined in FAR 52.227-7013.

The products described in this document may contain design defects or errors known as errata which may cause the product to deviate from published specifications. Current characterized errata are available on request.

The code names presented in this document are only for use by Intel to identify products, technologies, or services in development that have not been made commercially available to the public, i.e., announced, launched, or shipped. They are not "commercial" names for products or services and are not intended to function as trademarks.

Contact your local Intel sales office or your distributor to obtain the latest specifications and before placing your product order.

Copies of documents which have an order number and are referenced in this document, or other Intel literature may be obtained by calling 1-800-548-4725 or by visiting Intel's website at <http://www.intel.com/design/literature.htm>.

Intel processor numbers are not a measure of performance. Processor numbers differentiate features within each processor family, not across different processor families. See http://www.intel.com/products/processor_number for details.

Intel is a trademark of Intel Corporation or in the US and other countries.

* Other brands and names may be claimed as the property of others.

Copyright © 2016 Intel Corporation. All rights reserved.



Table of Contents

1	Document Scope	6
2	Background – WiGig System Operation	7
2.1	System Block Diagram	7
2.2	Beam Forming.....	8
2.3	TX Duty Cycle	8
2.4	Intel 18260NGW Module in Toshiba Model PT16B.....	8
3	Simulation Methodology	9
3.1	Assessment considerations.....	9
3.2	Near field and transition-zone field results.....	9
3.3	Simulation tool	9
3.3.1	Tool description.....	9
3.3.2	Solver description.....	10
3.3.3	Convergence criteria and power density calculations.....	10
3.4	Finding near field, worst-case simulation configuration	11
3.4.1	Terminology:	12
3.4.2	Primer on field vector representation.....	12
3.4.3	Domain search for worst-case direction	14
3.5	3D models used in the simulation.....	16
3.5.1	Worst-case operating conditions of the platform.....	16
3.5.2	RFEM 1 housing inside Intel 18260NGW module.....	17
3.5.3	Closest distance to the body of an end user.....	18
3.5.4	Metals in proximity of the RFEM 1	18
3.6	Antenna feed	19
4	Simulation Results	20
4.1.1	Upper-bound simulation results of the plane exposure	20
4.1.2	Single-point power density values with worst-case antenna phases for plane exposure.....	23
4.1.3	One dimensional cut of the mesh single-point power density for plane exposure.....	26
4.1.4	Integrated power density over 1 cm ² for plane exposure	27
4.1.5	Power density for plane exposure	29
4.2	Conclusion	32
5	Validation of Simulation Model in Transition-Zone Field to Far-Field	33
5.1	Correlation of E.I.R.P. in the near to far field.....	33
5.1.1	Far field boundary calculation.....	33
5.1.2	Test laboratory	34
5.1.3	Correlation of measurements and simulation	34
5.1.4	Estimated conducted power level	37
5.2	Simulating a canonical antenna design	38
6	Summary	41



List of Figures

Figure 1 – Intel 18260NGW module system block diagram	7
Figure 2 – Illustration of the Adaptive Mesh Technique	10
Figure 3 – Search plane is the x-y plane (i.e. the blue plane as illustrated in this picture)	11
Figure 4 – Near field worst-case terminology and orientation	12
Figure 5 – Platform operating modes – laptop mode	16
Figure 6 – Platform operating modes – tablet mode	16
Figure 7 – Platform picture with RFEM 1 location	17
Figure 8 – Platform picture with RFEM 1 location – tablet operating mode	17
Figure 9 – Platform planes touching the body in tablet mode	18
Figure 10 – Channel 1 upper-bound, single-point power density	21
Figure 11 – Channel 2 upper-bound, single-point power density mesh	21
Figure 12 – Channel 3 upper-bound, single-point power density mesh	22
Figure 13 – Footprint of single-point power density plane representation	22
Figure 14 – Channel 1 single-point power density mesh	24
Figure 15 – Channel 2 single-point power density mesh	24
Figure 16 – Channel 3 single-point power density mesh	25
Figure 17 – 1-dimensional plots of the power density on Channel 1	26
Figure 18 – 1-dimensional plots of the power density on Channel 2	26
Figure 19 – 1-dimensional plots of the power density on Channel 3	26
Figure 20 – Channel 1 worst case – integrated power over 1cm ² and platform	27
Figure 21 – Channel 2 worst case – integrated power over 1cm ² and platform	28
Figure 22 – Channel 3 worst case – integrated power over 1cm ² and platform	28
Figure 23 – Footprint of integrated power density plane	29
Figure 24 – HFSS Simulation results in Channel 1	29
Figure 25 – HFSS Simulation results in Channel 2	30
Figure 26 – HFSS Simulation results in Channel 3	30
Figure 27 – Antenna dimensions in mm	33
Figure 28 – Comparison of E.I.R.P. simulation to lab measurements – channel 1	34
Figure 29 – Comparison of E.I.R.P. simulation to lab measurements – channel 2	35
Figure 30 – Comparison of E.I.R.P. simulation to lab measurements – channel 3	35
Figure 31 – Estimate conducted power from E.I.R.P. data	37
Figure 32 – Simulation of a single patch antenna	38
Figure 33 – Patch antenna gain	38
Figure 34 – Simulation 3D structure	39
Figure 35 – Power density of canonical patch antenna	40

List of Tables

Table 1 – Acronyms	5
Table 2 – WiGig Channels Frequencies	20
Table 3 – Phases configurations for the worst case	23
Table 4 – Worst-case power density	31
Table 5 – Fraunhofer distance from each channel	34
Table 6 – Gain calculation from power density per several distances	39
Table 7 – Summary of simulation results for RF exposure compliance	41

**Table 1 – Acronyms**

ABS	Acrylonitrile butadiene styrene
Ant	Antenna
Az	Azimuth
BB	Base Band
BF	Beam Forming
BT	Bluetooth
BW	Band Width
CAD	Computer Aided Design
CPU	Central Processing Unit
E.I.R.P.	Equivalent Isotropically Radiated Power
El	Elevation
EM	Electro-Magnetic
GHz	Giga Hertz
IF	Intermediate Frequency
MAC	Media Access Control
M.2	M2: Formerly known as Next Generation Form Factor (NGFF); used as specification for connectors of the expansions cards mounted on computer
mmWave	Milli-Meter Wave
OTP	One Time Programmable memory
PC	Personal Computer
R&D	Research and Development
RF	Radio Frequency
RFEM	Radio Front End Module
RFIC	Radio Frequency Integrated Circuit
RX	Receive
SKU	Stock Keeping Unit, specific product model version
TPC	Transmit Power Control
T/R SW	Transmit / Receive Switch
TX	Transmit
WiGig	Wireless Gigabit Alliance – the alliance that promoted the 60GHz into 802.11ad standard.



1 Document Scope

This report is submitted to support the compliance to FCC rule located in Title 47 of the Code of Federal Regulations (CFR) parts §2.1093 and §15.255(g), of Intel 18260NGW WiGig module (FCC ID: PD918260NG), including an active antenna array, embedded inside the Toshiba Model PT16B platform.

Please note that the Toshiba model PT16B is the regulatory model number. This host is also marketed under the name Altair. In this report, we refer only to it as the model PT16B.

Per the location of the active antenna array (a.k.a. RFEM 1) in the Toshiba model PT16B platform, the distance between the antenna arrays to the body of an end user, at the closest contact point, will be in the near field. At this time power density measurements are not possible.

Therefore, to obtain an estimation of the near field power density results, we used an EM simulation that includes the RFEM 1 transmitter model, embedded inside the Toshiba model PT16B. The simulation method and the simulation results are described in this document.

Due to the lack of standardized code validation, benchmarking and uncertainty of the simulation software, the near field¹ to far field results are included for the purpose of providing confidence for the software simulation model used and that the results produced were within an acceptable range when compared with the measured results. The error margins of all test results have been considered collectively by the FCC to determine compliance.

To prove the validity of these results, this report shows how the results of the same simulation are correlated to lab measurements for transition-zone field² to far field distances.

Chapter 2 provides relevant background on Intel 18260NGW module. Chapter 3 describes the simulation methodology to determine RF exposure (power density) levels. Chapter 4 includes simulation results, and Chapter 5 describes the correlation between simulation and lab measurements in transition-zone field to far field^{3,4}. Chapter 6 summarizes the RF-Exposure analysis.

Please note that this document covers non-confidential parts information, relevant details and explanations that qualify for confidentiality are included separately in the test report document entitled "Intel model 18260NGW embedded inside Toshiba model PT16B – WiGig subsystem theory of operation Revision 1.1"; therefore, not included in this report. However, in this document some places make cross-reference to the confidential Operational Description exhibit for details about device operation.

¹ The "near field" nomination is used to indicate the reactive near field zone at antenna proximity particularly the field in the exposure plane. In this report it is the zone between 0 and 5 cm.

² The transition-zone field nomination is used to indicate the radiative near field zone in which the correlation between the measurement and simulation is performed i.e, it is the zone between 5cm and 12 cm

³ The Far field zone nomination is used to indicate the zone above 10cm from the antenna.

⁴ The far field lower distance (12 cm) is determined according to the RFEM 1 dimension. The transition-zone field is the zone going from the lower limit of the measurement distance (5 cm) to the far field lower limit (12 cm).

2 Background – WiGig System Operation

2.1 System Block Diagram

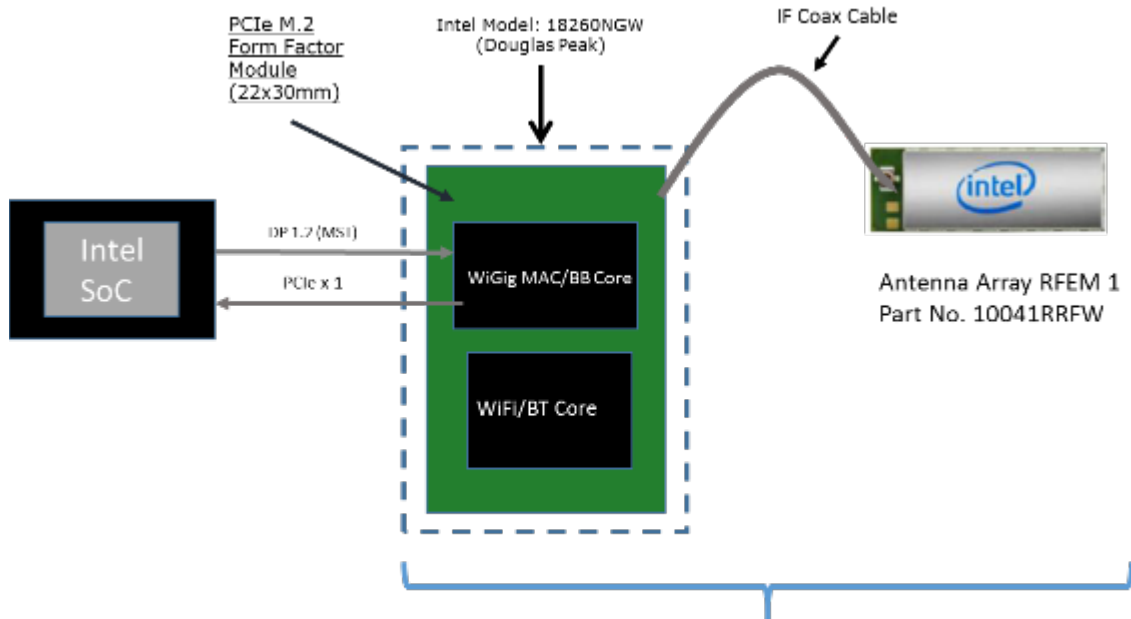
Intel 18260NGW module (FCC ID: PD918260NG) is a solution for embedded WiGig connectivity for various PC client as well as modern 2 in 1 detachable platforms. For this RF exposure evaluation the Intel 18260NGW module will be incorporated into the Toshiba model PT16B. The Toshiba PT16B is a 2 in 1 PC that can be used in traditional portable laptop mode or converted to a tablet mode.

The client solution for Toshiba PT16B includes the 18260NGW WiGig module (FCC ID: PD918260NG) connected to a beamforming antenna array RFEM 1 using one IF coaxial cable.

The WiGig module (FCC ID: PD918260NG) is a PCIe M.2 module consisting of a WiGig BB chip, which implements the WiGig MAC, Modem, BF algorithm, and active antenna array module control, as well as the BB + IF stage circuitry. This WiGig module re-uses the same WiGig MAC/BB silicon core as the previous generation module 17260NGW (FCC ID: PD917260NG).

RFEM 1 (10041RRFW) is an active antenna array module, which converts the IF signal to 60GHz signal. It also performs the beamforming functionality by phase shifting the RF signal that goes to each antenna. The RFEM 1 is slave to the WiGig BB chip since all module control and algorithms run on the BB chip.

Intel System-on-Chip (SoC) houses the CPU (central processing unit) which executes different applications, as well as provides the command and control of the client solution, including all I/O data and addressing.



Client Solution includes Douglas Peak module
IF Coax Cable and antenna array RFEM 1 (10041RRFW)

Figure 1 – Intel 18260NGW module system block diagram



The RFEM 1 is located at the top of the lid of the platform, in order to improve the RF propagation of the communication link.

2.2 Beam Forming

Achieving high bandwidth communication over 60GHz channels usually requires directional antenna at the transmitter and receiver sides. In consumer electronics, fixed directional or mechanically rotated antenna are not practical and electronically steerable antenna are usually used.

In Intel 18260NGW module, such electronic steerable antenna array is being used. Beam forming protocol (defined in the standard ISO/IEC/IEEE 8802-11:2012/Amd.3:2014(E), Clause 21) is used to find the right direction for setting both the RX and TX antenna directions.

Due to the RFEM 1 structure it is not easy to predict the direction and beam forming combination that yields the maximum energy in near field. To find this value a search over the possible beam forming combination was made and the worst case value was taken. Detailed explanation of this process can be found in section 3.4.

2.3 TX Duty Cycle

The WiGig protocol, as defined in ISO/IEC/IEEE 8802-11:2012/Amd.3:2014(E), Clause 21, is packet based with time division multiplexing (TDM). Intel 18260NGW module is configured to guarantee that the TX-Duty-Cycle, defined as the ratio of the duration of all transmissions to the total time, is at most 70% over any 10 seconds period. This was established by worst case analysis, as derived from full system simulation, and verified by measurements.

The limited TX-Duty-Cycle is established based on HW and FW implementation with ~100 ms (102.4 ms) measurement duration and 10 seconds averaging; other details are provided in the Operational Description exhibit. The 70% duty cycle limitation is guaranteed independent of user activity, and therefore it adheres to the source-based time-averaging definition in Title 47 of the Code of Federal Regulations (CFR) 2.1093(d)(5).

In addition, measurements of the Intel 18260NGW module configured to obtain maximal TX-Duty-Cycle in a fully loaded system, resulted in actual maximum TX-Duty-Cycle of 58% over any 10 seconds period, lower than the upper bound derived from the analysis in this section.

2.4 Intel 18260NGW Module in Toshiba Model PT16B

Intel produces several HW SKUs (variations) of Intel 18260NGW module, which target different types of customer platform products.

Toshiba uses Intel 18260NGW module inside the Toshiba Model PT16B platform. This SKU is characterized by:

1. supporting channels 1+2+3
2. Reduced power emission, which translates to:
 - a. Maximum transmit conducted power of 5.5 dBm aggregated conducted power at the antenna ports.
 - b. Maximum TX duty-cycle of 70%.



3 Simulation Methodology

3.1 Assessment considerations

During the system operation mode it is challenging to define a practical system worst case scenario in which the user is exposed to the highest emission level. To ensure coverage of the highest emission the analysis of the worst case corner condition is used and is emphasized in the following:

1. Platform orientation with respect to human body – In most of the cases when the platform is very close to the human body, and the energy is directed to the human body, the human body will attenuate the signal. In this case, a reliable link can't be achieved. When a reliable link can't be maintained, the system enters search mode. In search mode, the system will transmit a low-duty cycle of less than 1%. This search mode contains signals which happen every 100ms at the maximum output power. However, in the analysis done for this document, the system is simulated in operational mode (not in search mode), operating at 70% duty cycle, which is much higher than the search mode.
2. Energy direction, beam forming – In order to avoid human body attenuation or object blockage of a reliable link, the system beam forming will automatically search for a path that will establish a more reliable link. So, in real life, in most of the cases the EM path will not be directed towards the human body. However, in the analysis presented in this document, worst-case beam forming direction is used.

Please note that the above worst case assessment description is very conservative in that it is very unlikely this case would happen under normal usage conditions. Since we cannot state with 100% certainty that this is impossible, we kept this worst case assessment methodology. We ask that this be taken into consideration.

3.2 Near field and transition-zone field results

Finding the worst-case emission in the near field across the platform boundary requires searching on two orthogonal domains. One domain is the location – the need to find the place that has the worst case energy. The other domain that has to be searched is the antenna phases – the need to search over the various antenna phases and find the antenna phase combination that gives the worst-case value. Section 3.4 explains how these two worst-case (location and phase) searches are investigated.

After the completion of the worst case phase analysis, the phases found during this analysis are used to find the worst case integrated energy across 1cm^2 averaging area for RF exposure evaluation purposes. EM simulation is used for this analysis.

Transition-zone field to far field analysis is both simulated and correlated against measured lab results.

3.3 Simulation tool

3.3.1 Tool description

For the EM simulation, the commercially available ANSYS Electronics Desktop 2016 (HFSS) is used. The ANSYS HFSS tool is used in the industry for simulating 3-D, full-wave electromagnetic fields. Intel uses this EM simulation tool due to its gold-standard accuracy, advanced solver, and high-performance computing technology capabilities for doing accurate and rapid design of high-frequency components.

3.3.2 Solver description

The HFSS simulation is performed using the Finite Element Method, which operates in the frequency domain. The HFSS is based on an accurate direct solver with first order basis functions.

3.3.3 Convergence criteria and power density calculations

The HFSS uses a volume air box containing the simulated area to calculate the EM fields. The box is truncated by a PML (Perfect Match Layer) boundary condition. The simulation uses the adaptive mesh technique (see Figure 2) to meet the exit criteria of $\Delta S < 0.02$. The ΔS is the change in the magnitude of the S-parameters between two consecutive passes, if the magnitude and phase of all S-parameters change by an amount less than the Maximum Delta S per Pass value from one iteration to the next, the adaptive analysis stops.

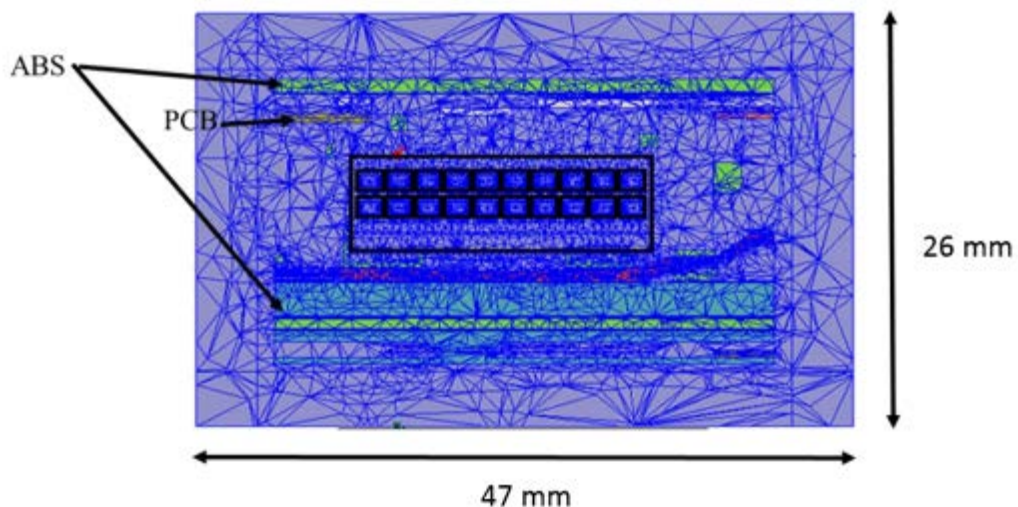


Figure 2 – Illustration of the Adaptive Mesh Technique

After having the simulated electrical and magnetic (E and H) fields at each point in the mesh, the Poynting vector is calculated. The integrated power density on a given surface is calculated as the surface integral of the Poynting vector:

$$W = \frac{1}{2} \operatorname{Re} \int_S (\vec{E} \times \vec{H}^*) \cdot \vec{n} dS$$

Notes:

1. HFSS phasors in field calculator are peak phasors which leads to the $\frac{1}{2}$ factor in the Poynting vector calculation.
2. Figure 2 is an illustration of the adaptive mesh technique and is presented in the context of simulation methodology presentation.

3.4 Finding near field, worst-case simulation configuration

As explained previously, near-field analysis requires finding the worst-case location (along the searched plane) and antenna phase values. As further explained, the search should be done on two domains:

- 1) Look for the worst-case position (across the search plane).
- 2) Look for the worst-case antenna phases

Note: the search plane here is defined as the plane that is used for the calculation of the worst-case antenna phase values. This is the x-y plane that is adjacent to the platform outer plastic (at the location of the RFEM 1) and represents the worst-case scenario where the user is the closest to the platform.

Simulated plane on the platform edge



Figure 3 – Search plane is the x-y plane (i.e. the blue plane as illustrated in this picture)

Note that for the xyz coordinate references used throughout this report, we always consider the z-axis as being towards the body direction. This consideration is used to conserve a general consistency for the field's representation, and calculations in the worst-case determination procedure detailed below. In summary, the xy plane is the exposure plane, and the z-axis is the vector in propagation direction towards the body.

3.4.1 Terminology

- Element – Each one of the radiating elements that are used in the system. (The antenna array has 16 radiating elements.) We denote the antenna element with index \mathbf{k} in this explanation.
- \mathbf{N} – Number of chains in the RFEM 1, $\mathbf{N}=16$.
- Point – Each point on the grid that is used for searching for the worst- case position. The points are spaced 0.1mm from each other. The grid point would be denoted as \mathbf{g} in this explanation.
- Complex E field vector generated by the \mathbf{k}^{th} antenna element at point \mathbf{g} :

$$\overrightarrow{E_{k,g}} = \vec{x}(\text{Re}[E_{kx,g}] + j\text{Im}[E_{kx,g}]) + \vec{y}(\text{Re}[E_{ky,g}] + j\text{Im}[E_{ky,g}]) + \vec{z}(\text{Re}[E_{kz,g}] + j\text{Im}[E_{kz,g}])$$
- Complex H field vector generated by the \mathbf{k}^{th} antenna element at point \mathbf{g} :

$$\overrightarrow{H_{k,g}} = \vec{x}(\text{Re}[H_{kx,g}] + j\text{Im}[H_{kx,g}]) + \vec{y}(\text{Re}[H_{ky,g}] + j\text{Im}[H_{ky,g}]) + \vec{z}(\text{Re}[H_{kz,g}] + j\text{Im}[H_{kz,g}])$$
- \hat{x} , \hat{y} , \hat{z} – are unit direction vectors having unit magnitude and are mutually orthogonal to each other.
- Without loss of generality in this explanation, RFEM 1 and search plane are in the \hat{x} , \hat{y} plane and the integrated 1cm^2 plane is perpendicular to \hat{z} direction.

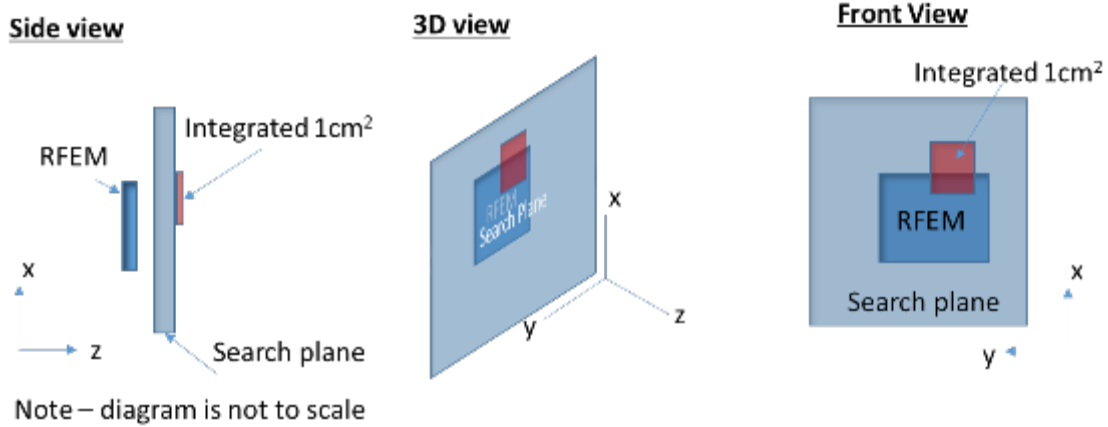


Figure 4 – Near field worst-case terminology and orientation

3.4.2 Primer on field vector representation

E and H fields generated by the \mathbf{k} chain are

$$\overrightarrow{E_k} = \vec{x}(\text{Re}[E_{kx}] + j\text{Im}[E_{kx}]) + \vec{y}(\text{Re}[E_{ky}] + j\text{Im}[E_{ky}]) + \vec{z}(\text{Re}[E_{kz}] + j\text{Im}[E_{kz}])$$

$$\overrightarrow{H_k} = \vec{x}(\text{Re}[H_{kx}] + j\text{Im}[H_{kx}]) + \vec{y}(\text{Re}[H_{ky}] + j\text{Im}[H_{ky}]) + \vec{z}(\text{Re}[H_{kz}] + j\text{Im}[H_{kz}])$$

E and H fields generated by all \mathbf{N} chains are

$$\overrightarrow{E_{\text{All}}} = \vec{x} \sum_{k=1}^N (\text{Re}[E_{kx}] + j\text{Im}[E_{kx}]) + \vec{y} \sum_{k=1}^N (\text{Re}[E_{ky}] + j\text{Im}[E_{ky}]) + \vec{z} \sum_{k=1}^N (\text{Re}[E_{kz}] + j\text{Im}[E_{kz}])$$

$$\overrightarrow{H_{\text{All}}} = \vec{x} \sum_{k=1}^N (\text{Re}[H_{kx}] + j\text{Im}[H_{kx}]) + \vec{y} \sum_{k=1}^N (\text{Re}[H_{ky}] + j\text{Im}[H_{ky}]) + \vec{z} \sum_{k=1}^N (\text{Re}[H_{kz}] + j\text{Im}[H_{kz}])$$



The Poynting vector generated by all N chains is

$$\begin{aligned}
 \overrightarrow{P_{\text{General,All}}} &= \frac{1}{2} \overrightarrow{E_{\text{All}}} \times \overrightarrow{H_{\text{All}}^*} \\
 &= \frac{1}{2} \left\{ \vec{x} \left\{ \sum_{k=1}^N (\text{Re}[E_{ky}] + j\text{Im}[E_{ky}]) \sum_{k=1}^N (\text{Re}[H_{kz}] - j\text{Im}[H_{kz}]) \right. \right. \\
 &\quad - \sum_{k=1}^N (\text{Re}[E_{kz}] + j\text{Im}[E_{kz}]) \sum_{k=1}^N (\text{Re}[H_{ky}] - j\text{Im}[H_{ky}]) \Big\} \\
 &\quad + \vec{y} \left\{ \sum_{k=1}^N (\text{Re}[E_{kz}] + j\text{Im}[E_{kz}]) \sum_{k=1}^N (\text{Re}[H_{kx}] - j\text{Im}[H_{kx}]) \right. \\
 &\quad - \sum_{k=1}^N (\text{Re}[E_{kx}] + j\text{Im}[E_{kx}]) \sum_{k=1}^N (\text{Re}[H_{kz}] - j\text{Im}[H_{kz}]) \Big\} \\
 &\quad + \vec{z} \left\{ \sum_{k=1}^N (\text{Re}[E_{kx}] + j\text{Im}[E_{kx}]) \sum_{k=1}^N (\text{Re}[H_{ky}] - j\text{Im}[H_{ky}]) \right. \\
 &\quad - \sum_{k=1}^N (\text{Re}[E_{ky}] + j\text{Im}[E_{ky}]) \sum_{k=1}^N (\text{Re}[H_{kx}] - j\text{Im}[H_{kx}]) \Big\}
 \end{aligned}$$

Power flow is

$$\begin{aligned}
 \text{Re}[\overrightarrow{P_{\text{General,All}}}] &= \frac{1}{2} \left\{ \vec{x} \left\{ \sum_{k=1}^N \text{Re}[E_{ky}] \sum_{k=1}^N \text{Re}[H_{kz}] + \sum_{k=1}^N \text{Im}[E_{ky}] \sum_{k=1}^N \text{Im}[H_{kz}] - \sum_{k=1}^N \text{Re}[E_{kz}] \sum_{k=1}^N \text{Re}[H_{ky}] \right. \right. \\
 &\quad - \sum_{k=1}^N \text{Im}[E_{kz}] \sum_{k=1}^N \text{Im}[H_{ky}] \Big\} \\
 &\quad + \vec{y} \left\{ \sum_{k=1}^N \text{Re}[E_{kz}] \sum_{k=1}^N \text{Re}[H_{kx}] + \sum_{k=1}^N \text{Im}[E_{kz}] \sum_{k=1}^N \text{Im}[H_{kx}] - \sum_{k=1}^N \text{Re}[E_{kx}] \sum_{k=1}^N \text{Re}[H_{kz}] \right. \\
 &\quad - \sum_{k=1}^N \text{Im}[E_{kx}] \sum_{k=1}^N \text{Im}[H_{kz}] \Big\} \\
 &\quad + \vec{z} \left\{ \sum_{k=1}^N \text{Re}[E_{kx}] \sum_{k=1}^N \text{Re}[H_{ky}] + \sum_{k=1}^N \text{Im}[E_{kx}] \sum_{k=1}^N \text{Im}[H_{ky}] - \sum_{k=1}^N \text{Re}[E_{ky}] \sum_{k=1}^N \text{Re}[H_{kx}] \right. \\
 &\quad - \sum_{k=1}^N \text{Im}[E_{ky}] \sum_{k=1}^N \text{Im}[H_{kx}] \Big\}
 \end{aligned}$$



3.4.3 Domain search for worst-case direction

The two domain search is completed as follows:

- A. First find a direction (location) for the worst-case 1cm² square averaging area using upper bound methods.

The basic concept behind the upper bound method is to assume that there could be an “ideal beam forming” mechanism that could align the phases of all the elements for both E and H fields. (Obviously, in real life this cannot happen. This is the reason that this is an upper-bound method). When this ideal mechanism is used, then all the complex phasors are aligned to the same phase, hence the phasor absolute value can be used instead of the phasor. The E (and H) field for any direction is the sum of the magnitude of the fields (look at item 3, below, for a more formal description).

This method provides the worst-case position independent of the antenna phases. It allows finding the worst-case location with this “ideal beam forming” mechanism.

Item 3, below, translates the above verbal description into more formal mathematical wording.

- B. After the worst-case direction is found using the upper bound method, the antenna phases are aligned to this direction. The antenna phases are aligned to maximize the power across the 1cm² averaging area that was found using the upper bound method. The method that is used to find the required antenna phases is as follows: first order the antenna according to the power contribution on the found 1cm² from the highest to the lowest. Then start by activating the antenna that contributes the most, set its phase to 0, and then activate the 2nd antenna and search over the phases for the 2nd antenna. Choose the phase that maximizes the power of the two antenna elements. For finding the phase for the third antenna, fix antenna 1's phase to zero and antenna 2's phase to the value that was found before. Then search for the phases for the third antenna that maximize the power. Continue with the same process until you reach the 16th element.
- C. Calculate the power density with the antenna phases that were found in the previous item (item B).

The above process can be written as the following algorithm:

1. A grid is defined with 0.1mm spacing.
2. At each point in the grid, the complex E and H fields are calculated using each one of the 16 radiating elements, separately. Each one of the calculated E and H fields are 3D complex vectors, so the simulation output from this stage is 16 3D complex E field strength vectors and 16 3D complex H field strength vectors. The vectors are defined as:

$$\overrightarrow{E_{k,g}} = \vec{x}(\operatorname{Re}[E_{kx,g}] + j\operatorname{Im}[E_{kx,g}]) + \vec{y}(\operatorname{Re}[E_{ky,g}] + j\operatorname{Im}[E_{ky,g}]) + \vec{z}(\operatorname{Re}[E_{kz,g}] + j\operatorname{Im}[E_{kz,g}]) \text{ and}$$
$$\overrightarrow{H_{k,g}} = \vec{x}(\operatorname{Re}[H_{kx,g}] + j\operatorname{Im}[H_{kx,g}]) + \vec{y}(\operatorname{Re}[H_{ky,g}] + j\operatorname{Im}[H_{ky,g}]) + \vec{z}(\operatorname{Re}[H_{kz,g}] + j\operatorname{Im}[H_{kz,g}])$$

3. Upper-bound assumption is used to derive the E and H field on each one of the grid points. The following items describe the upper bound method that is used:
 - a. The calculation is made separately for E field and H field.
 - b. For E field, the following calculation is made independently for each one of the grid points:



$$\begin{aligned}\overrightarrow{E_{UB,g}} = & \vec{x} \sum_{k=1}^N \sqrt{\operatorname{Re}[E_{kx,g}]^2 + \operatorname{Im}[E_{kx,g}]^2} + \vec{y} \sum_{k=1}^N \sqrt{\operatorname{Re}[E_{ky,g}]^2 + \operatorname{Im}[E_{ky,g}]^2} \\ & + \vec{z} \sum_{k=1}^N \sqrt{\operatorname{Re}[E_{kz,g}]^2 + \operatorname{Im}[E_{kz,g}]^2} = \vec{x} \sum_{k=1}^N |E_{kx}| + \vec{y} \sum_{k=1}^N |E_{ky}| + \vec{z} \sum_{k=1}^N |E_{kz}| \end{aligned}$$

The magnitude of the complex E vector is summed over the antenna elements. The summation is done for each one of the grid points, and for each one of the elements in each direction, independently.

- c. The output of the previous item is the 3D real vector of the E field on each one of the simulated grid points in each direction. The physical implementation is that an ideal beam forming was done for the E field for each one of the points.
- d. The same process as described in item b is done for the H field.

$$\begin{aligned}\overrightarrow{H_{UB,g}} = & \vec{x} \sum_{k=1}^N \sqrt{\operatorname{Re}[H_{kx,g}]^2 + \operatorname{Im}[H_{kx,g}]^2} + \vec{y} \sum_{k=1}^N \sqrt{\operatorname{Re}[H_{ky,g}]^2 + \operatorname{Im}[H_{ky,g}]^2} \\ & + \vec{z} \sum_{k=1}^N \sqrt{\operatorname{Re}[H_{kz,g}]^2 + \operatorname{Im}[H_{kz,g}]^2} = \vec{x} \sum_{k=1}^N |H_{kx,g}| + \vec{y} \sum_{k=1}^N |H_{ky,g}| + \vec{z} \sum_{k=1}^N |H_{kz,g}| \end{aligned}$$

- e. At each point in the grid, the Poynting vector is calculated by vector multiplication of the E and H fields, which are added up in items b and d. As explained before, without a loss of generality, we assume that the search plane is the x/y plane. All three (xyz) components of the Poynting vector are added, and not just the component that is normal to the x/y plane:

$$\begin{aligned}P_g &= \frac{1}{2} \operatorname{Re}\{(\vec{E} \times \vec{H}^*)\} = \frac{1}{2} \operatorname{Re}\left\{\left(\left((E_y H_z^* - E_z H_y^*)\right) \hat{x} + \left((E_z H_x^* - E_x H_z^*)\right) \hat{y} + \left(E_x H_y^* - E_y H_x^*\right) \hat{z}\right)\right\} \\ P_{g,x} &= \frac{1}{2} \operatorname{Re}\{E_y H_z^* - E_z H_y^*\} \\ P_{g,y} &= \frac{1}{2} \operatorname{Re}\{(E_z H_x^* - E_x H_z^*)\} \\ P_{g,z} &= \frac{1}{2} \operatorname{Re}\{E_x H_y^* - E_y H_x^*\}\end{aligned}$$

$$PUpperBound_g = \sqrt{P_{g,x}^2 + P_{g,y}^2 + P_{g,z}^2}.$$

- 4. The above calculated Poynting vectors are used to estimate the power across 1cm² area.

$$P1cm2 = \iint_{1cm^2} PUpperBound_g x, y, z$$

- 5. The 1cm² area with the highest power value is used as the worst-case direction. The antenna phases are aligned to maximize the energy in this 1cm² area, as explained below:

- a. Turn on each element one-by-one to find order of power intensity in the 1cm² window. (Find the order of contribution)
- b. Sort in the power order from the highest to the lowest, #0 to #15.
- c. Turn on #0 with phase P0=0. (reference)
- d. Turn on #1 and change the phase to maximize the power and find the phase P1.
- e. Keep P0 and P1 on, then turn on #2 and do same.
- f. Repeat for the rest of the antennas.
- 6. Using the antenna phases that were calculated in step 5, the power density is calculated along the exposure plane and then integrated across a 1cm² area.

3.5 3D models used in the simulation

3.5.1 Worst-case operating conditions of the platform

The Toshiba model PT16B is a platform with the ability to be used in two modes: laptop (Figure 5) or tablet (Figure 6). The worst case exposition to the radio frequency radiation can happen when the body of the user is in contact with the platform. The exposure plane illustrated in Figure 6 represents the worst-case condition in the tablet operating mode.



Figure 5 – Platform operating modes – laptop mode



Figure 6 – Platform operating modes – tablet mode

3.5.2 RFEM 1 housing inside Intel 18260NGW module

The 3D Intel 18260NGW module is simulated inside the Toshiba PT16B platform in order to obtain the most accurate results of the RF exposure. The Figure below shows that the RFEM 1 active antenna is located inside the lid at the top right of the screen.



Figure 7 – Platform picture with RFEM 1 location

As described in the section 3.5.3, the worst-case condition is the tablet operating mode. Figure 8 shows the position of the RFEM 1 antenna, as well as the main antenna beam direction.

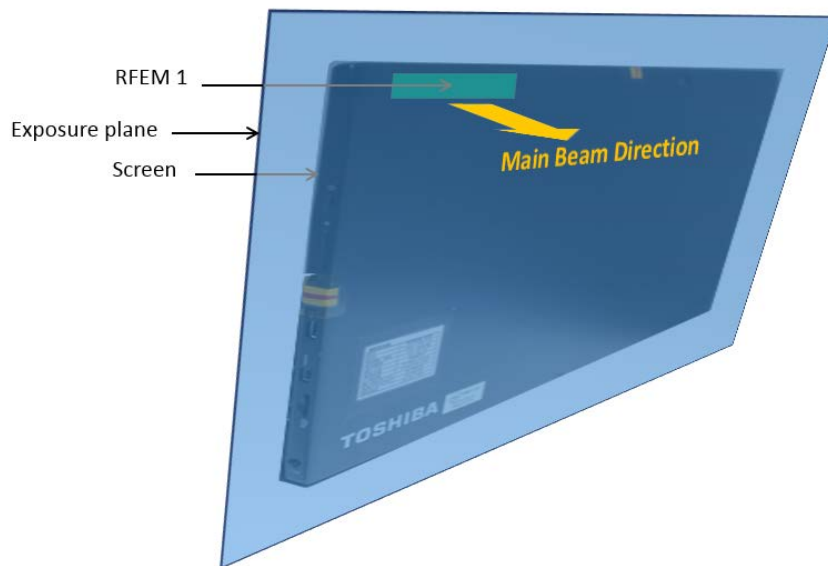


Figure 8 – Platform picture with RFEM 1 location – tablet operating mode

3.5.3 Closest distance to the body of an end user

In operating mode, the closest distance between the active antennas to the skin of an end user is when the person is holding the unit and touching the rear cover of the platform (at the exposure plane, shown in blue in Figure 9). In this case, the distance between a hand or body and the active antenna is between 1.5 mm and 1.7 mm. Figure 9 shows a cross section of the top of lid with the RFEM 1 inside the platform.



Figure 9 – Platform planes touching the body in tablet mode

3.5.4 Metals in proximity of the RFEM 1

All the metals that are in the RFEM 1 region (10mm on each side) were included in the simulation.



3.6 Antenna feed

This section provides a general description of the numerical simulations; other details of the simulation geometry are included in the confidential Operational Description exhibit. The EM simulation uses an accurate 3D model of the RFEM 1 antenna. The model includes the antenna elements as well as their feeding lines.

In the simulation (as well as in the product), each antenna element is fed independently, and we excite the antennas at the origin of the antenna structure on the RFEM 1 (the antenna structure includes the vias, traces, and antenna element).

Signals of equal phase and amplitude are applied to the feed points of individual array elements and the aggregate conducted equivalent power to all array elements is 5.5 dBm, thus each element is fed by -6.8 dBm (5.5 dBm divided over 16 elements). The trace loss from the feed point to the antenna is fully modeled and simulated. This via feed point is used as the interface point for the simulation. All antenna structures are fully simulated, including all parts of the PCB and antennas: conducted traces, feeds, antenna elements and dielectrics.

The total power (same per element) is used to build the pattern of radiated power through beam forming. For building the beamforming pattern the same power is used per element, while phase is changed per element, please look at section 2.2 for more information about the beamforming. Phases are derived for each excitation separately, to simulate the worst-case condition. Section 3.4 explains how the phases are derived to find the worst case condition.



4 Simulation Results

As described in the section 3.5.3, a plane has been simulated. The power density results of the plane are presented in this section.

The power density has been simulated over three channels with frequencies listed in **Table 2**. For each channel, we'll present the resulting details according to the methodology explained in section 3.4:

- Simulation results of the single-point power density for each single-point across the Mesh ($P_{UpperBound_g}$) and the worst-case coordinates. Please note that this value represents single-point power density and not integrated power density over 1cm^2 . (Even though a 1mW/cm^2 scale is used, this value represents an upper-bound power density for each single point of the mesh, which is much smaller area than 1cm^2 .)
- The results of the single-point power density using the antenna phases corresponding to the worst-case coordinates found.
- A 1-dimensional cut of the mesh single-point power density – Showing a 1-dimensional cut of the mesh power density. In the xy plane, the x cut is made with the y at the maximum value; similarly, the y cut is made with the x at the maximum value. These results show the results using the xyz components of the Poynting vector.
- Integrated power density over 1cm^2 – These figures present the integrated power density across 1cm^2 using the xyz components of the Poynting vector. Each point in the figure represents integration over 1cm^2 , where the point location is the location of the center of the square.
- The worst-case power density, integrated over 1cm^2 using the worst-case antenna phases as computed by the simulation using the xyz components of the Poynting vector.

Table 2 – WiGig Channels Frequencies

	Channel 1	Channel 2	Channel 3
Frequency (GHz)	58.32	60.48	62.64

4.1.1 Upper-bound simulation results of the plane exposure

The Figure 10, Figure 11 and Figure 12 present upper-bound, single-point power density as described in section 3.4.

In each one of the figures, the worst case 1cm^2 is plotted in the figure, and the coordinate of the center of the 1cm^2 is given (0,0 for the co-ordination system is lower left corner of the plots). Please note that since the worst-case conditions are searched over a plane for near field, then the azimuth and the elevation are not relevant. The worst case position is calculated using all the power density single-points issued from the upper-bound simulation results. The upper-bound, worst-case power density distributions for three channels are shown in Figure 10, Figure 11 and Figure 12. We leverage the phase conditions (summarized in Table 3) for each antenna element that resulted in these worst-case conditions to evaluate final integrated power density. The mathematical basis for using these as the worst-case phase conditions to evaluate the final integrated power density is provided in section 3.4.3.

The plane dimensions of the single-point power density results is 30 mm x 20 mm (Figure 10, Figure 11 and Figure 12).

The footprint of the platforms components in the plane for single-point power density representation is showed in Figure 13.

Worst-case coordinates on channel 1 are $X = -0.33$ cm, $Y = -0.11$ cm

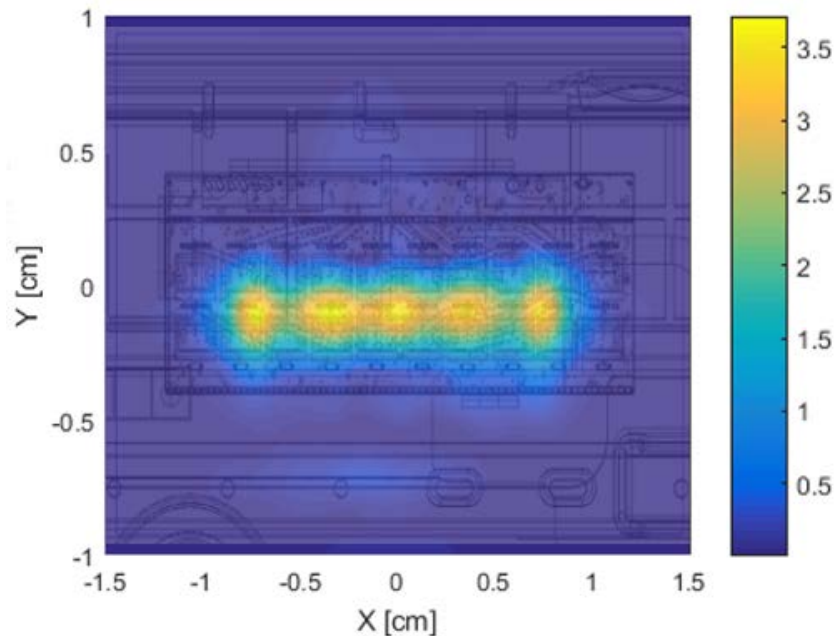


Figure 10 – Channel 1 upper-bound, single-point power density

Worst-case coordinates on channel 2 are $X = 0.01$ cm, $Y = -0.14$ cm.

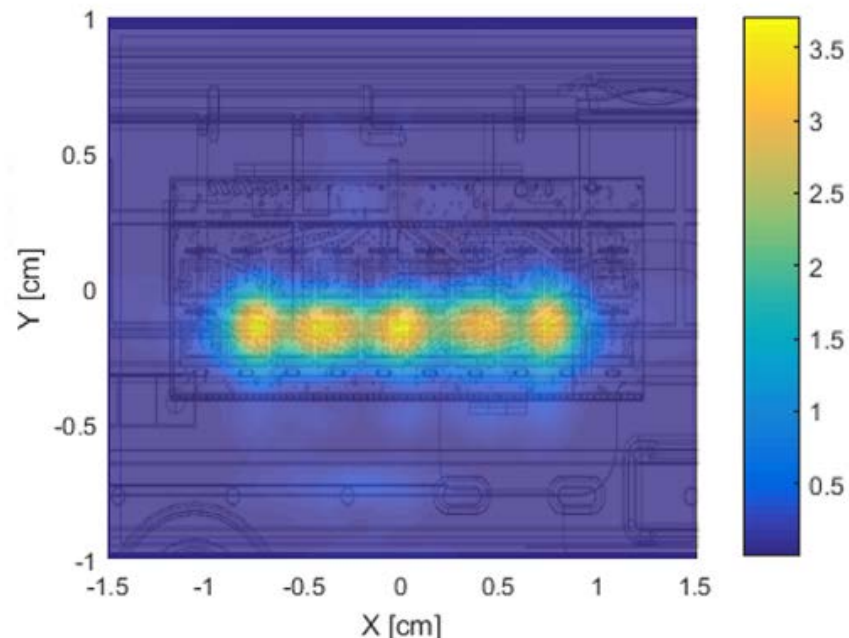


Figure 11 – Channel 2 upper-bound, single-point power density mesh

Worst-case coordinates on channel 3 are $X = -0.72$ cm, $Y = -0.19$ cm.

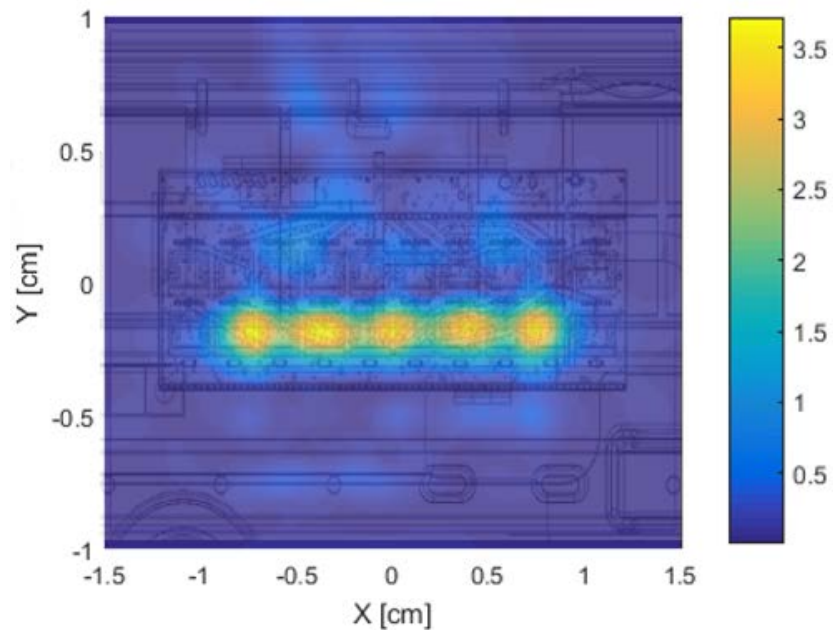


Figure 12 – Channel 3 upper-bound, single-point power density mesh

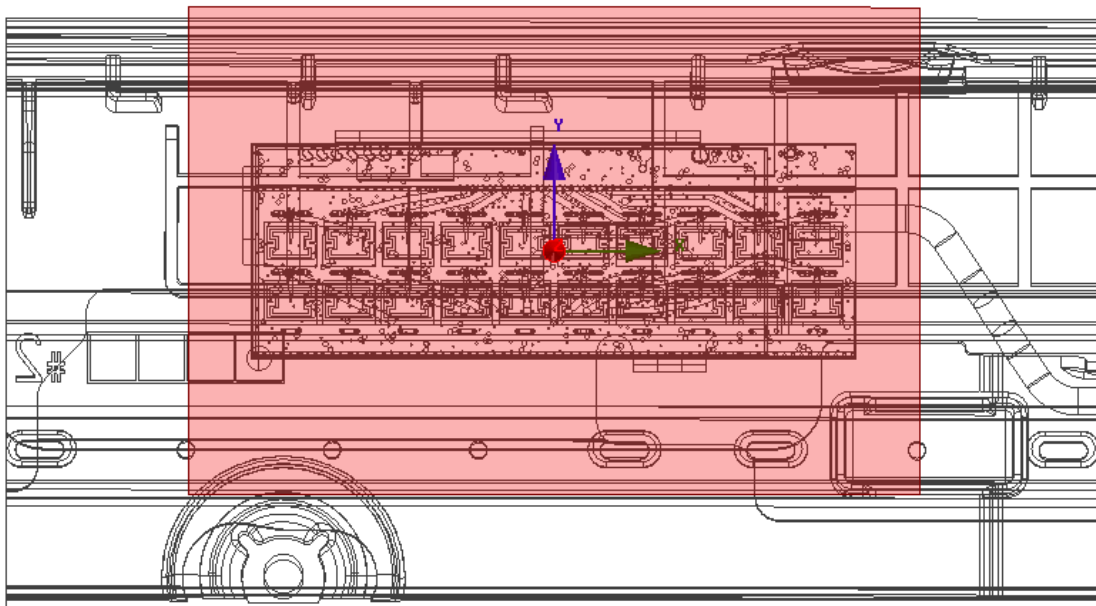


Figure 13 – Footprint of single-point power density plane representation

4.1.2 Single-point power density values with worst-case antenna phases for plane exposure

Table 3 shows the phase for each antenna element per channel for the worst case found as described in the section 3.4. The phases search algorithm is detailed in bullet 5 of section 3.4.3.

Antenna index	Phases [Degrees]		
	Channel 1	Channel 2	Channel 3
0	270	135	90
1	0	180	90
2	0	180	315
3	0	45	0
4	45	0	0
5	225	135	45
6	90	45	0
7	135	270	45
8	45	135	270
9	45	225	135
10	90	135	0
11	0	45	0
12	225	0	90
13	45	135	45
14	0	0	0
15	180	180	0

Table 3 – Phases configurations for the worst case

The amplitude on each antenna is -6.8 dBm, as explained in section 3.6.

Figure 14, Figure 15, and Figure 16 present power density in the body direction using the worst-case antenna phases presented in Table 3. The simulated power density area has a size of 30 mm x 20 mm.

Worst-case coordinates on channel 1 are $X = -0.86$ cm, $Y = 0.02$ cm.

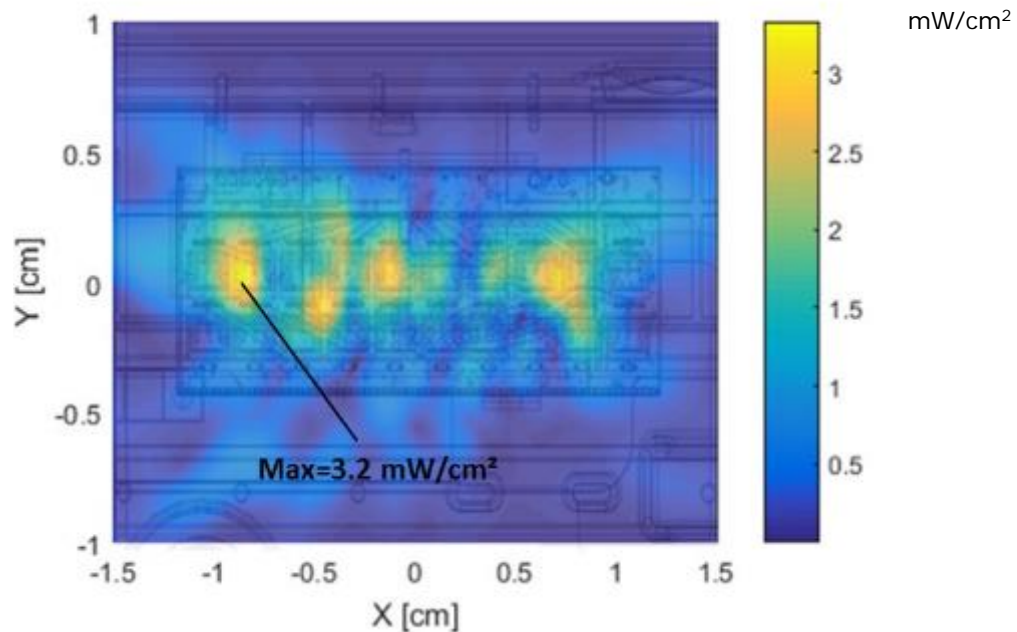


Figure 14 – Channel 1 single-point power density mesh

Worst-case coordinates on channel 2 are $X = -0.57$ cm, $Y = -0.12$ cm.

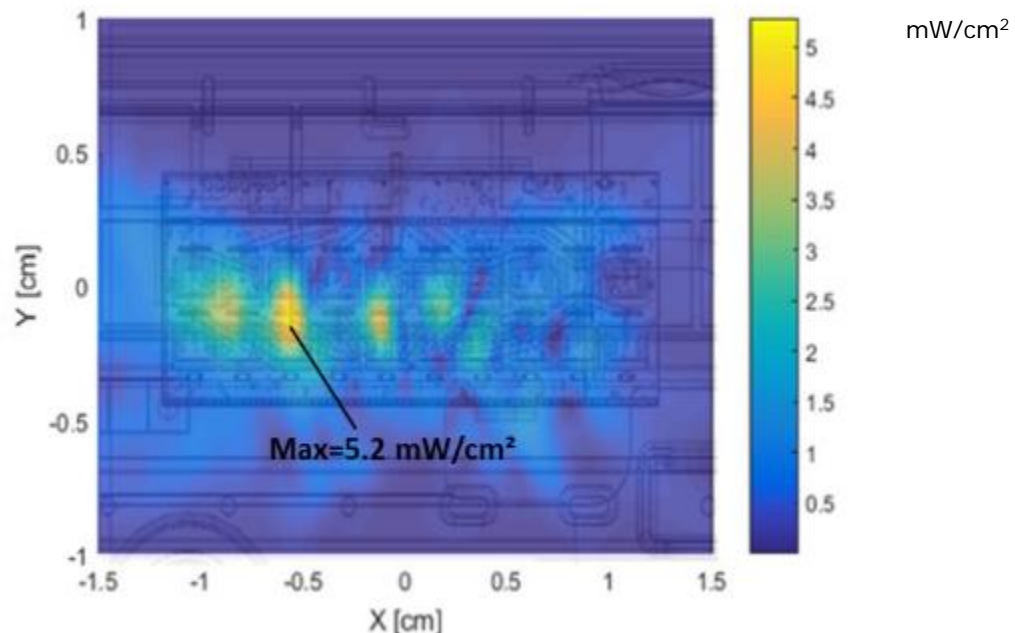


Figure 15 – Channel 2 single-point power density mesh

Worst-case coordinates on channel 3 are $X = 0.32$ cm, $Y = -0.22$ cm.

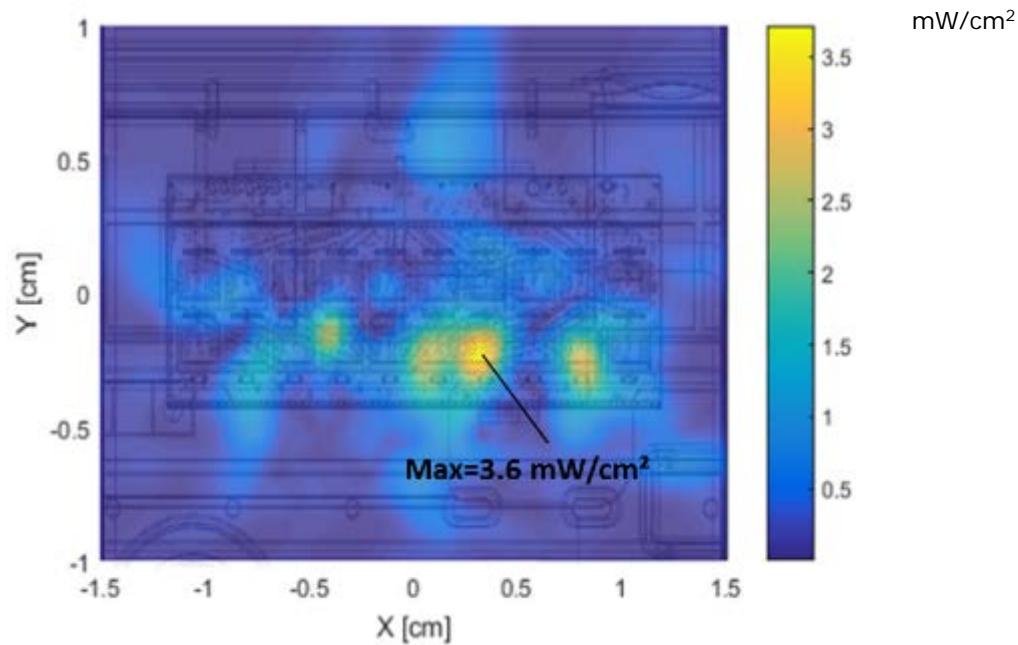


Figure 16 – Channel 3 single-point power density mesh

The highest value shown in these figures is a point and not yet integrated over the 1cm^2 . The final power density value is given in section 4.1.5.

4.1.3 One dimensional cut of the mesh single-point power density for plane exposure

In Figure 17, Figure 18, and Figure 19, we present a subset of the simulation results from the xyz components of single-point power density values with worst-case antenna phases (section 4.1.2). The subset is a 1-dimensional cut in the x-axis and y-axis that shows the behavior of the near field power density at zero distance.

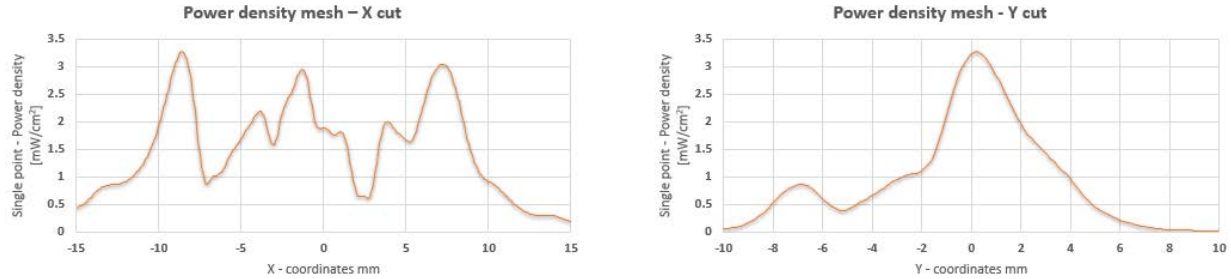


Figure 17 – 1-dimensional plots of the power density on Channel 1

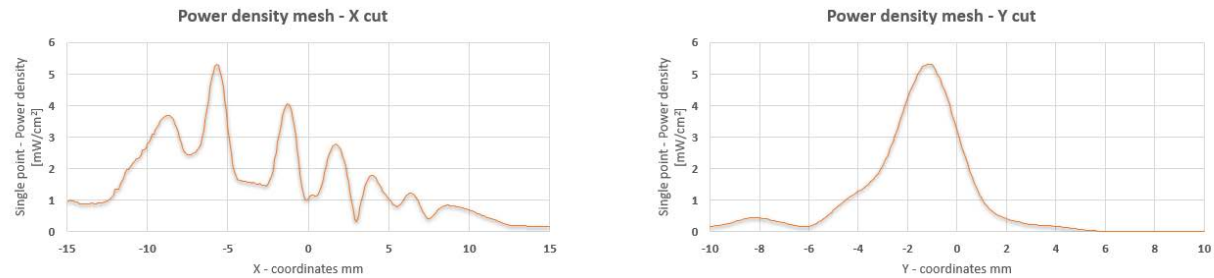


Figure 18 – 1-dimensional plots of the power density on Channel 2

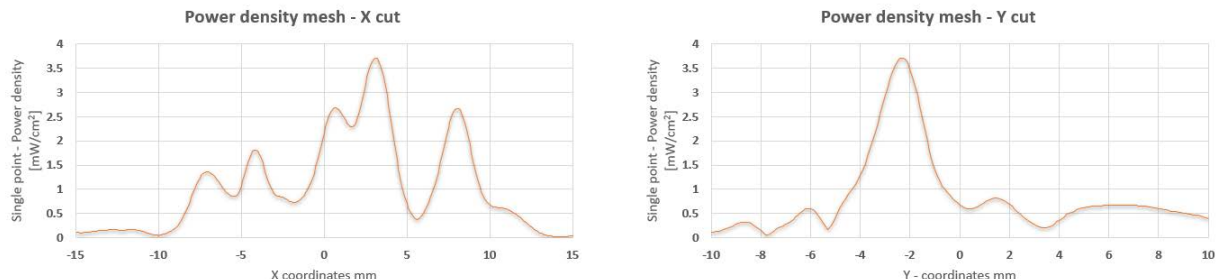


Figure 19 – 1-dimensional plots of the power density on Channel 3

4.1.4 Integrated power density over 1 cm² for plane exposure

Figure 20, Figure 21, and Figure 22 present the integrated power over 1cm² at 100% duty cycle for the worst-case scenario as explained in section 3.4.3. The plane dimensions of these results is 30 mm x 20 mm.

The 1cm² square location correspondent to the maximum of integrated power density value for each channel is plotted in yellow in Figure 20, Figure 21, and Figure 22. The maximum average values are mentioned in the second row of Table 4.

The footprint of the platform components in the plane for integrated power density representation is showed in Figure 23.

Worst-case coordinates on channel 1 are X = -0.55 cm, Y = 0cm.

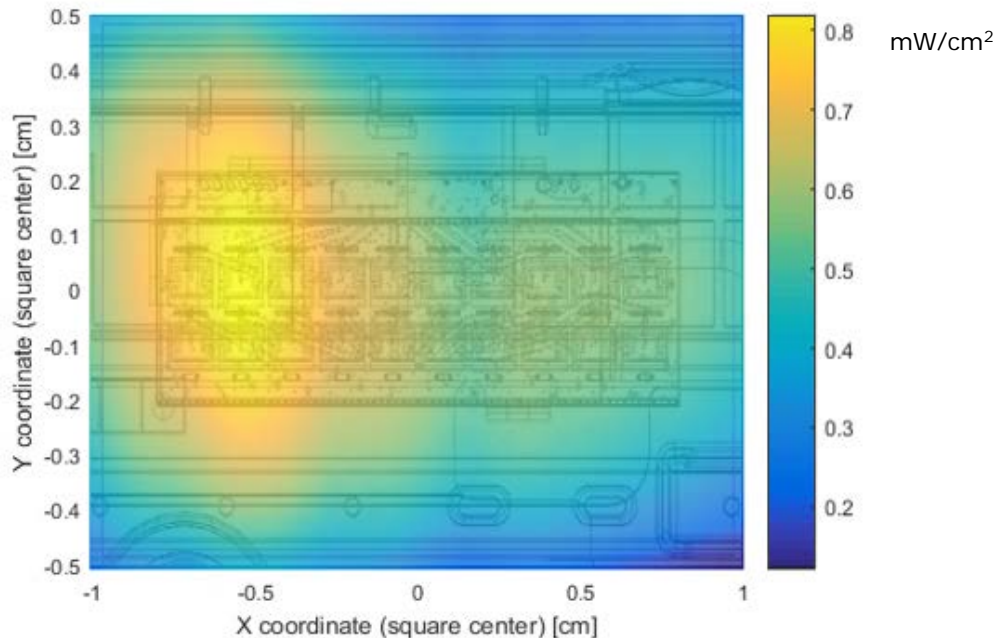


Figure 20 – Channel 1 worst case – integrated power over 1cm² and platform

Worst-case coordinates on channel 2 are $X = -0.59$ cm, $Y = -0.25$ cm

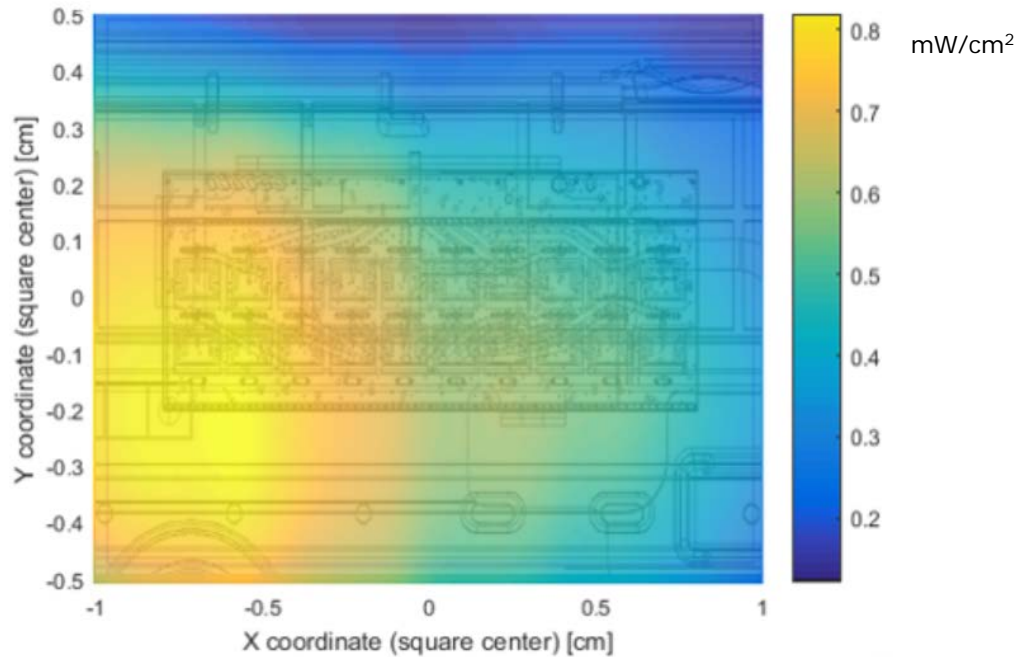


Figure 21 – Channel 2 worst case – integrated power over 1cm^2 and platform

Worst -case coordinates on channel 3 are $X = 0.44$ cm, $Y = -0.26$ cm

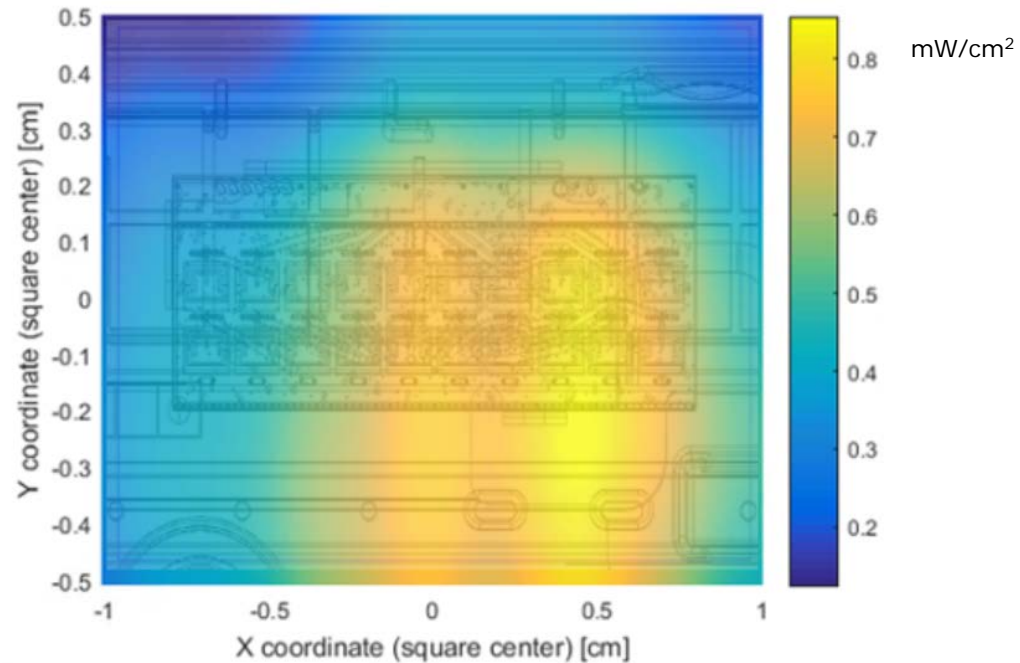


Figure 22 – Channel 3 worst case – integrated power over 1cm^2 and platform

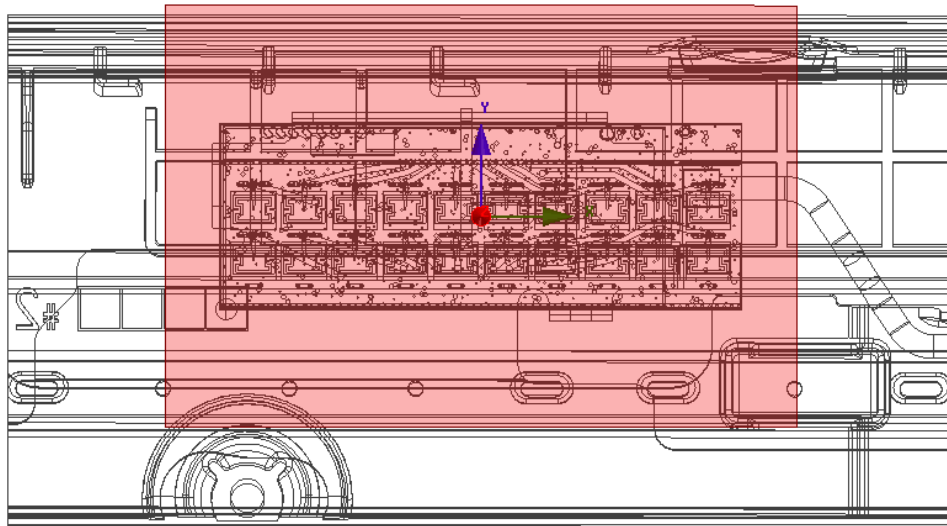


Figure 23 – Footprint of integrated power density plane

4.1.5 Power density for plane exposure

The Figure 24, Figure 25 and Figure 26 show the worst case power-density integrated over 1cm^2 versus the distance. As described in section 3.4.3 and section 3.5.2 the worst case was computed by the simulation using the worst case antenna phases. The 0mm reference correspond to the platform boundary, the active antenna located inside the platform is at 2 mm from this distance.

HFSS simulation results with 5.5 dBm conducted power
Channel 1 – Toshiba model TX20

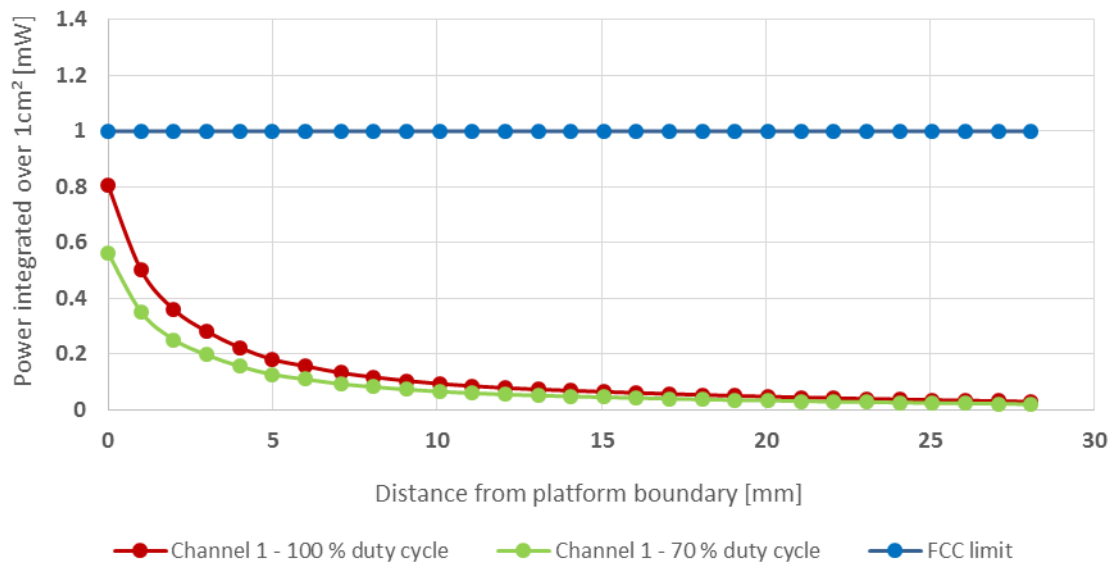


Figure 24 – HFSS Simulation results in Channel 1

HFSS simulation results with 5.5 dBm conducted power
Channel 2 – Toshiba model TX20

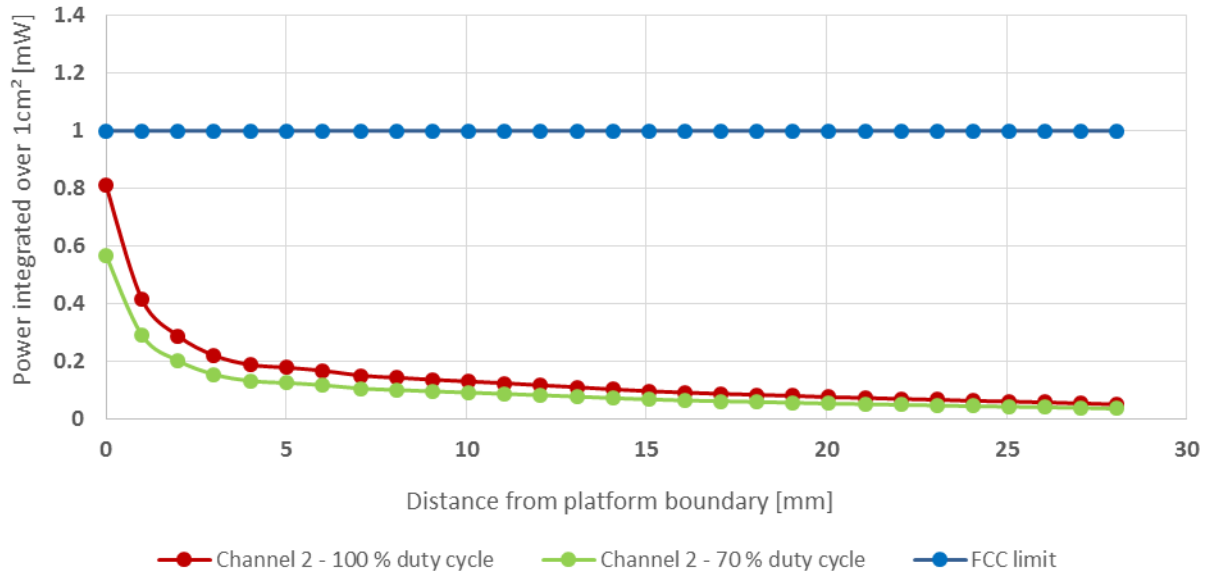


Figure 25 – HFSS Simulation results in Channel 2

HFSS simulation results with 5.5 dBm conducted power
Channel 3 – Toshiba model TX20

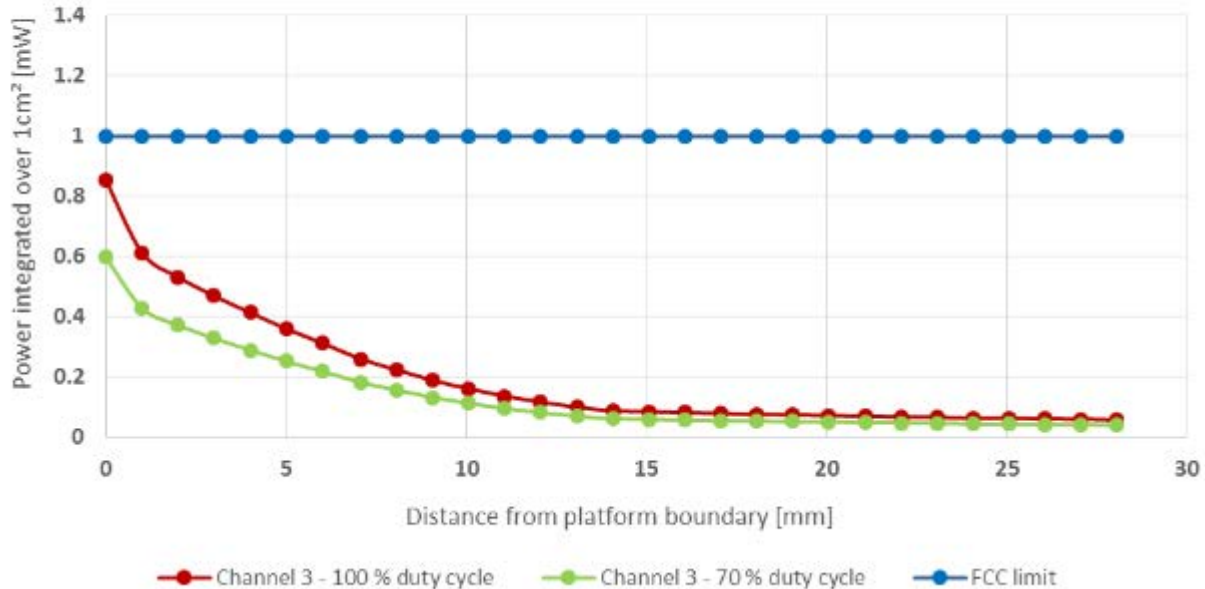


Figure 26 – HFSS Simulation results in Channel 3



The Table 4 shows the simulated worst-case power density at the plane area for each channels.

Highest power density	Channel 1 [mW/cm ²]	Channel 2 [mW/cm ²]	Channel 3 [mW/cm ²]
70% duty cycle	0.560	0.567	0.590
100% duty cycle	0.805	0.810	0.840

Table 4 – Worst-case power density

Notes for Table 4:

1. The worst-case channel is channel 3.
2. The Maximum power density (spatially integrated over worst 1cm²) in channel 3 is achieved at 0mm distance from the platform boundary and equals to 0.840mW/cm² over 100% duty cycle.
3. As explained in section 3.6, the Intel 18260NGW module is limited to transmit at a duty cycle of 70% over 10 seconds. Therefore the maximum spatially integrated and time averaged power density over 1cm² is $0.840 \times 0.7 = 0.590$ mW/cm².



4.2 Conclusion

The simulation results over one plane for three channels were presented in this report. The worst case has been shown on channel 3, with the maximum power density being 0.590 mW/cm^2 with three components. Note that the applicable FCC limit is 1 mW/cm^2 .

5 Validation of Simulation Model in Transition-Zone Field to Far Field

Due to the lack of standardized code validation, benchmarking and uncertainty estimations of the simulation software and the implemented device geometry, the near-field-to-far-field measurement results are included for the purpose of providing confidence for the software simulation model used and that the results produced were within an acceptable range when compared with the measured results. The error margins of all test results are requested to be considered collectively by the FCC to determine compliance.

To validate the accuracy of the simulation, we took a few metrics, presented in this chapter, including correlation of the simulated power density in the transition zone field to the far field against lab measurements. The same simulation was used for both power density estimation in the near field (Chapter4) and transition-zone field to far field correlation (this chapter).

5.1 Correlation of E.I.R.P. in the near to far field

Note that the correlation of E.I.R.P. in transition field to far field was done with a conducted output power of 6 dBm. This value was used for both lab measurements and simulation results.

5.1.1 Far field boundary calculation

Far field boundary can be estimated using *Fraunhofer distance* equation:

$$\text{Far FieldBoundary} = \frac{2d^2}{\lambda}$$

Equation 2 – Far field boundary calculation

In the RFEM 1, d (largest antenna dimension) = 19 mm (see Figure 27).

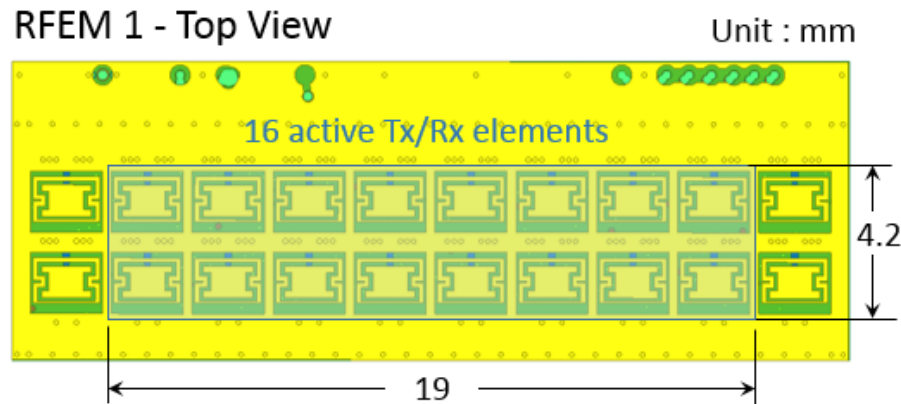


Figure 27 – Antenna dimensions in mm



Table 5 – Fraunhofer distance from each channel

Channel	λ (wave length) [mm]	Fraunhofer distance [cm]
1	5.14	12.07
2	4.96	12.62
3	4.79	12.91

5.1.2 Test laboratory

The measurements were done at the ISO 17025 accredited laboratory at Intel Mobile Communications France S.A.S. with FCC registration number #3478.01 on the Toshiba Model PT16B platform with 18260NGW module. Data can be found in the test report 160329-05.TR01, submitted with the application for this FCC ID.

5.1.3 Correlation of measurements and simulation

The figures in this section show E.I.R.P comparison simulation and measurements. The measured E.I.R.P. values from the test report 160329-05.TR01 are normalized to 100% duty cycle.

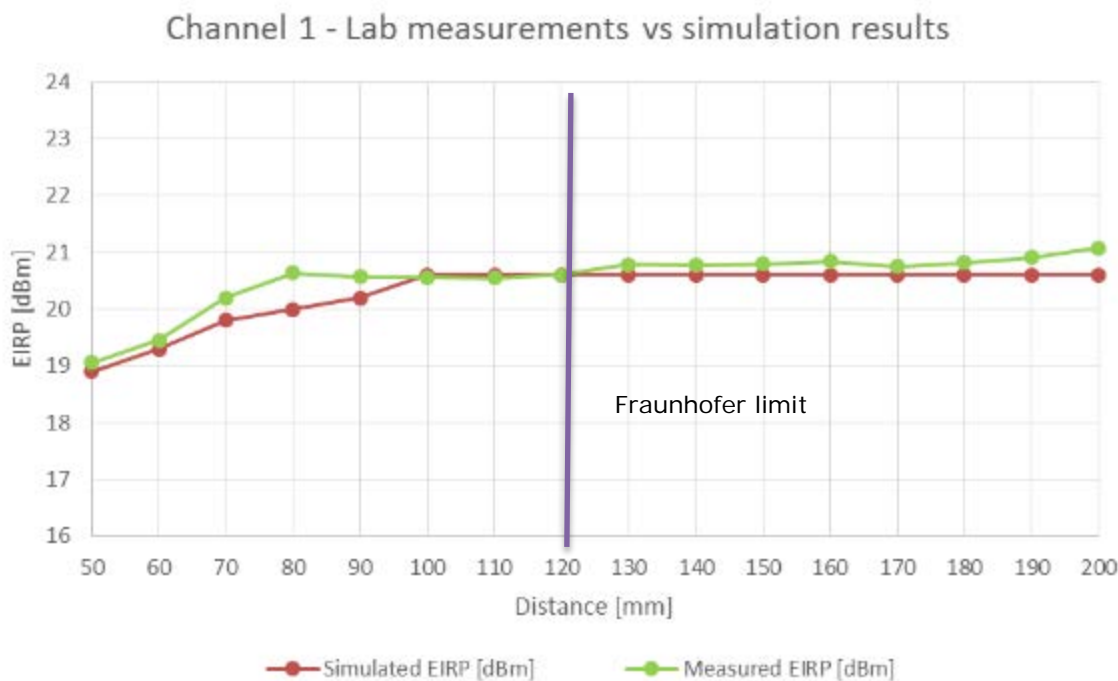


Figure 28 – Comparison of E.I.R.P. simulation to lab measurements – channel 1

Channel 2 - Lab measurements vs simulation results

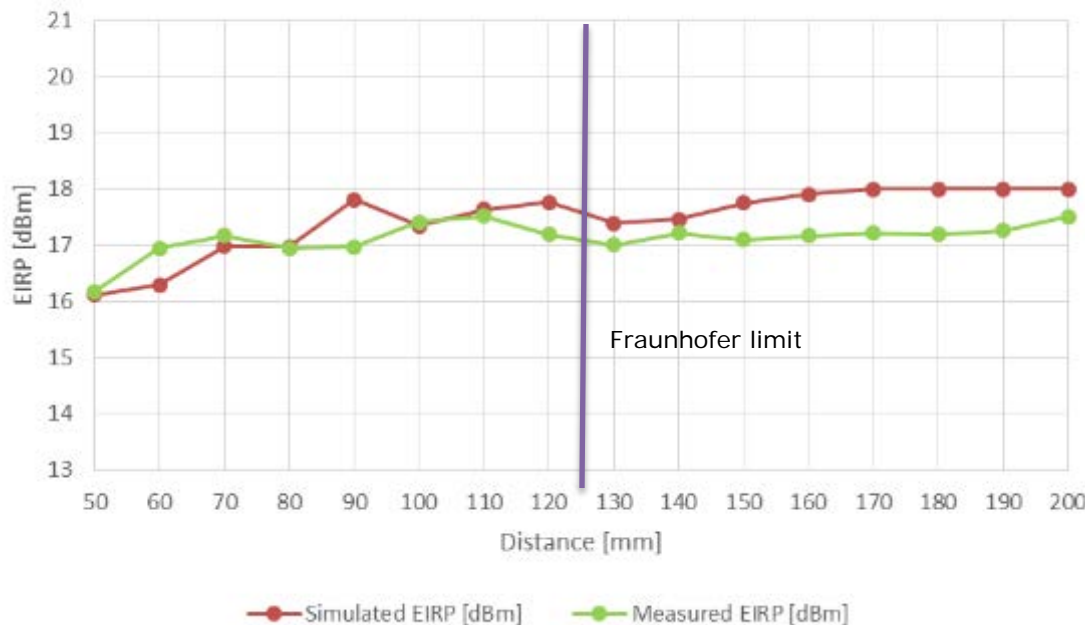


Figure 29 – Comparison of E.I.R.P. simulation to lab measurements – channel 2

Channel 3 - Lab measurements vs simulation results

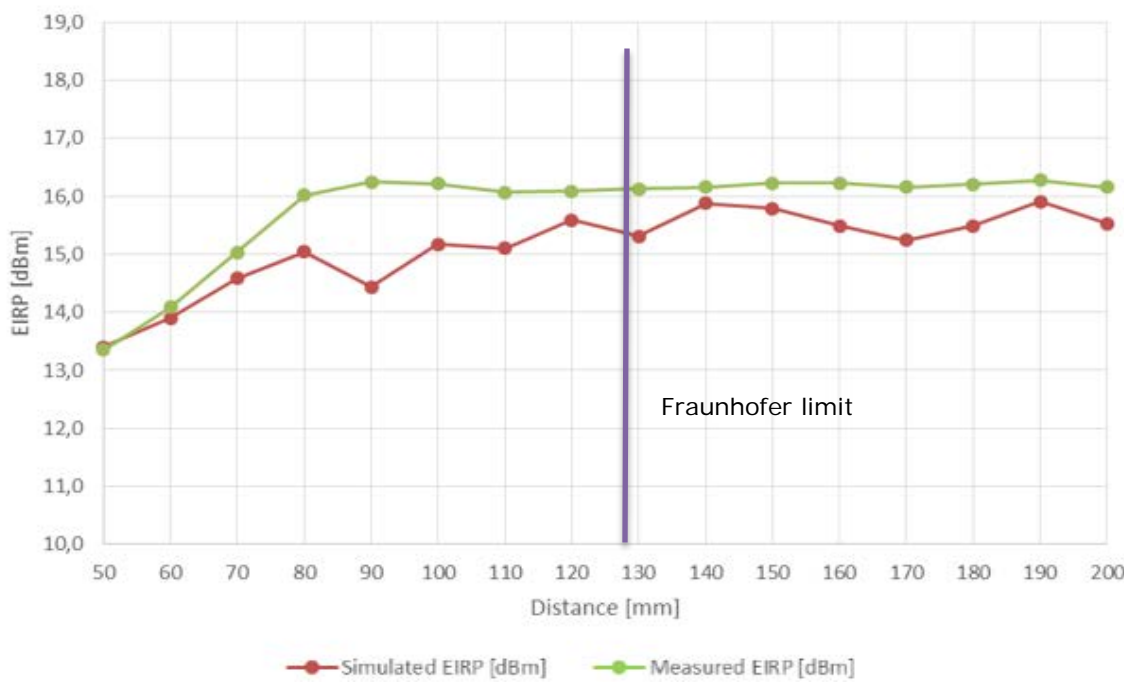


Figure 30 – Comparison of E.I.R.P. simulation to lab measurements – channel 3



The following observations can be made by looking at Figure 28, Figure 29 and Figure 30:

1. Measured E.I.R.P. increased to a steady state, demonstrating we are in the transition-zone field below 8cm (close to the Fraunhofer distance).
2. Good correlation can be seen in steady state power, with up to ~1.5dB difference between measured power and the simulated power.
3. Some difference can be seen in the energy build up between simulation results to lab measurements at close distances. This difference is probably due to near field effect and coupling between the platform to the antenna that is used for the measurements.

5.1.4 Estimated conducted power level

Measured E.I.R.P. signal power can be used to estimate the equivalent conducted power that is fed to the antenna array. The estimation is done by subtracting the antenna gain from the estimated E.I.R.P. level.

The E.I.R.P. level is the same as reported in previous section while the antenna gain is the antenna gain that is used in the 18260NGW modular approval.

Simulated antenna gain: Channel 1: 15.3dBi, Channel 2: 15.4dBi, Channel 3: 15dBi

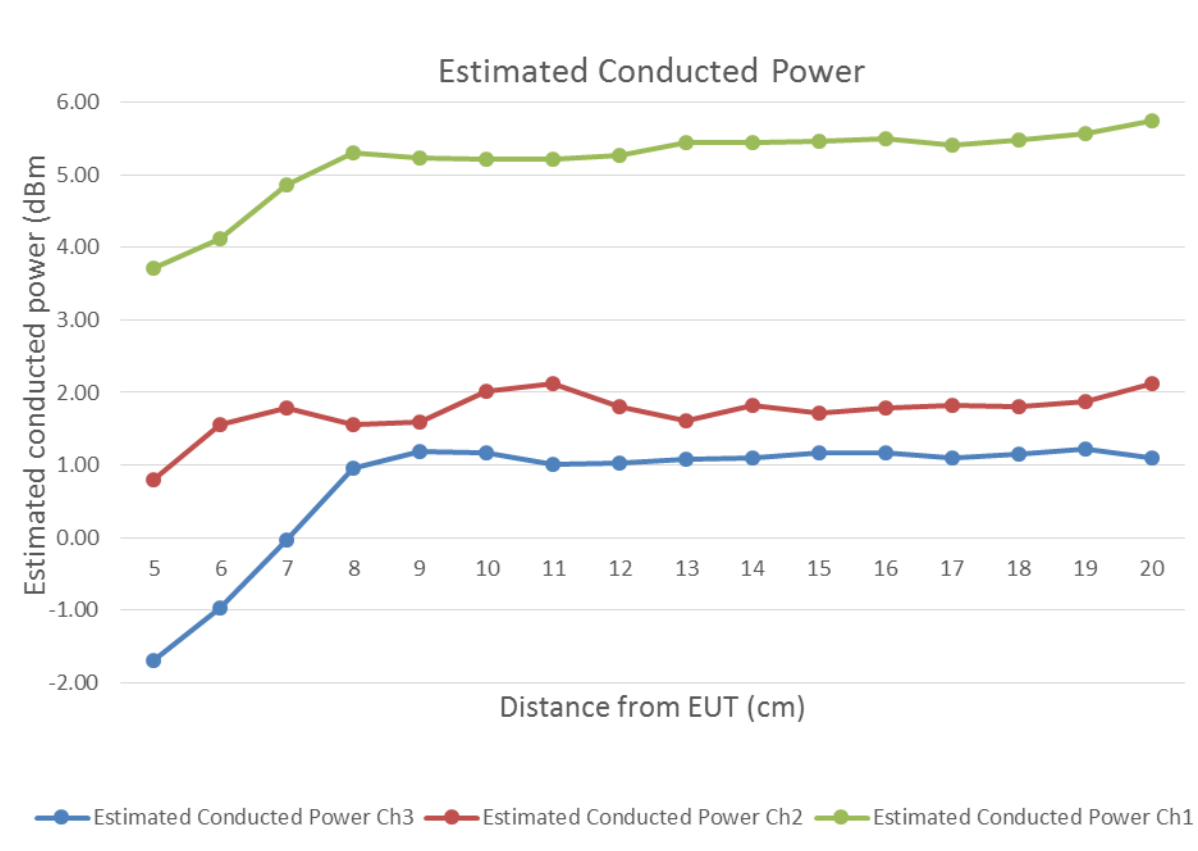


Figure 31– Estimate conducted power from E.I.R.P. data

Looking at Figure 31, one can see that the estimated conducted power is lower than the actual power level that was used. The tests were done with a conducted power of 5.5 dBm, while the estimated power for channels 1 is ~5.5 dBm, channel 2 is ~2.1 dBm, and channel 3 is ~1.1 dBm.

1. The antenna gain that is used for this estimation is the simulated antenna gain.
2. Lower estimated conducted power can be seen at short distances (up to about 8 cm) as coupling with the measuring device or other near objects. In addition at this range (5-8 cm), the antenna gain is lower than the far field antenna gain, hence E.I.R.P. is lower and the predicted power is lower.

5.2 Simulating a canonical antenna design

A simple patch antenna, with Length = 7.5mm (GND plane length) and Lambda = 4.8mm, which was designed to work at 62.5GHz, as can be seen in Figure 32.

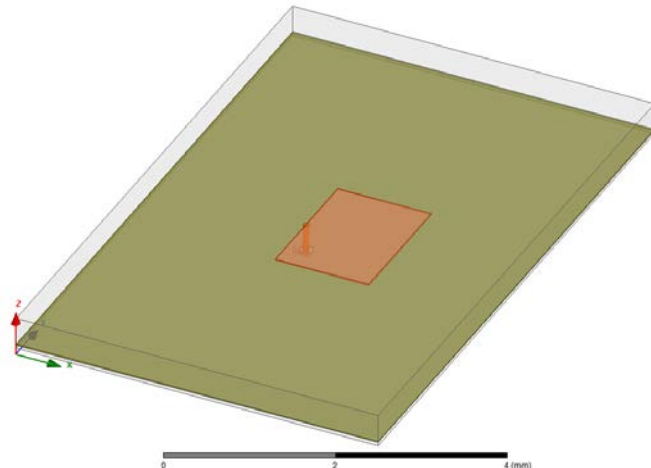


Figure 32 – Simulation of a single patch antenna

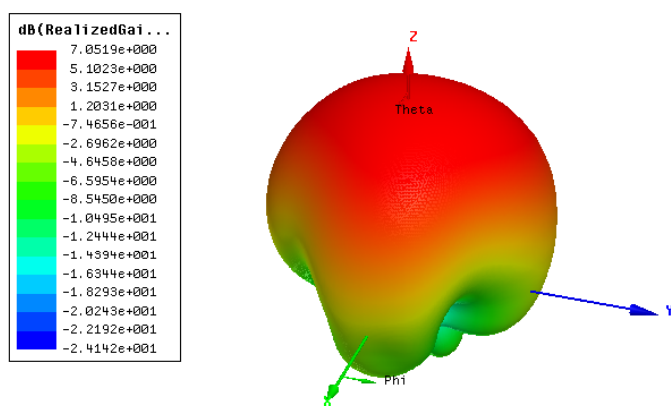


Figure 33 – Patch antenna gain

The simulated Far-Field Max Realized Gain [dBi] is 7.05[dBi], as simulated by far field simulation. The 7.05dBi gain was obtained using HFSS simulation with the Far Field Gain option.

Theoretically, the patch antenna gives ~7-9 dBi gain. The simulated patch antenna in the HFSS simulation is not a theoretical patch; it includes several “real life” non-idealities (width, size, feeding point, etc.). The 7.05 dBi Max Realized Gain is the gain obtained from HFSS simulation including those non-idealities.

A few test planes were integrated into the simulation at different far-field distances from the patch (shown below) for power density calculations:

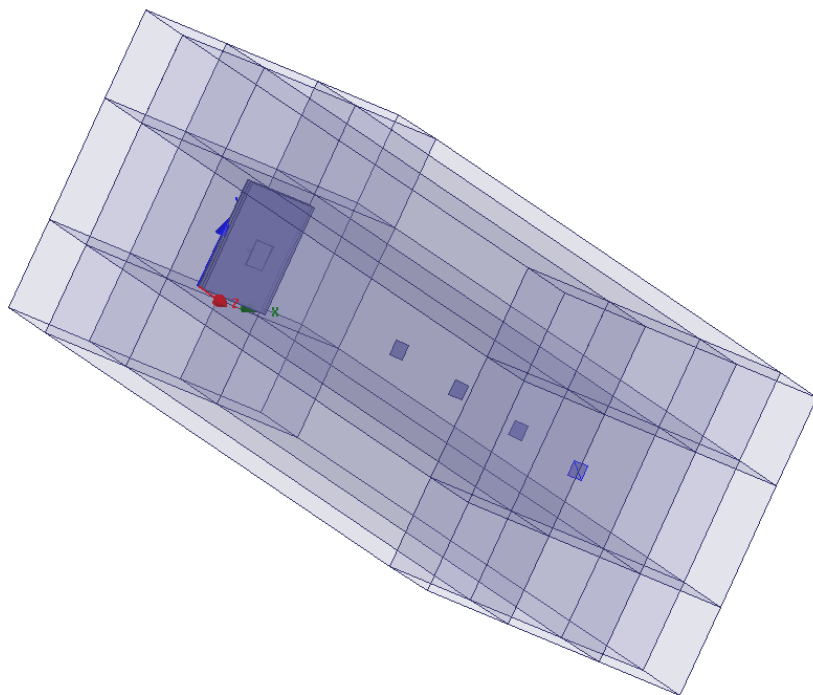


Figure 34 – Simulation 3D structure

The distances between the patch and the test planes range from 24mm to 54mm.

To validate the numerical tool, the power density results at the test planes are translated into gain using omnidirectional power propagation and compared to far field gain according to simulation (Table 6).

Table 6 summarizes the results.

Far Field Distance	$P_{omni} = \frac{P}{4\pi R^2} \left[\frac{W}{mm^2} \right]$	Power Density from simulation $\left[\frac{W}{mm^2} \right]$	Gain calculation from power density [dBi]
24mm	1.34e-4	6.70e-4	6.99
29mm	9.11e-5	4.61e-4	7.04
34mm	6.59e-5	3.38e-4	7.10
44mm	3.91e-5	2.03e-4	7.15
54mm	2.59e-5	1.35e-4	7.17

Table 6 – Gain calculation from power density per several distances

In Table 6, P is the simulated radiated power and R is the distance from the patch to the test plane.



Table 6 shows excellent correlation between the patch antenna gain calculated from power density, to the Far-Field Max realized gain (7.05[dBi]). This is also depicted in Figure 35 – Power density of canonical patch Figure 35.

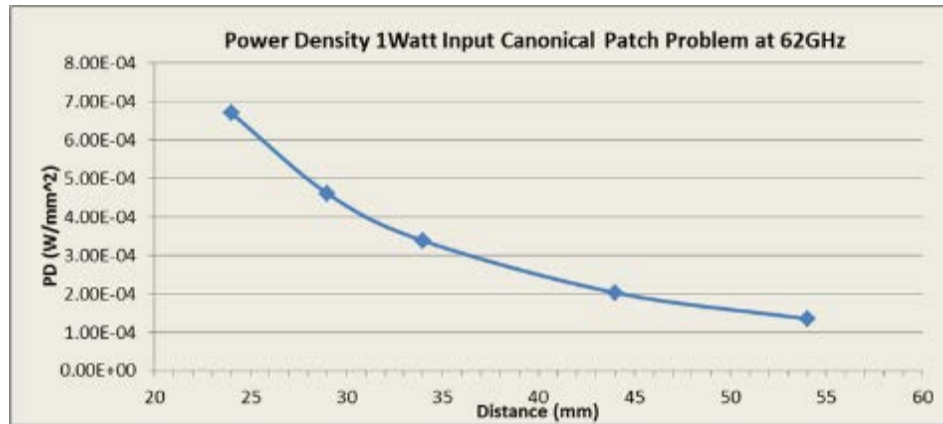


Figure 35 – Power density of canonical patch antenna



6 Summary

Due to the lack of standardized code validation, benchmarking, and uncertainty of the simulation software, the near-field-to-far-field results are included for the purpose of providing confidence in both the software simulation model used, and that the results produced were within an acceptable range when compared with the measured results. The error margins of all test results have been considered collectively by the FCC to establish confidence for the accuracy of the HFSS simulation.

Table 7 summarizes the simulation results in the near field of the Intel 18260NGW module, embedded in Toshiba Model PT16B:

Parameter	Value
Total conducted power	5.5 dBm
Maximum TX duty-cycle	70%
Maximum spatially integrated power density over 1cm ²	0.590 mW/cm ²

Table 7 – Summary of simulation results for RF exposure compliance

Therefore Intel 18260NGW module, embedded in Toshiba Model PT16B, complies with FCC rule located in Title 47 of the Code of Federal Regulations (CFR) parts §2.1093 and §15.255(g).